Registration Guided Simulation of Prostate Movement for Radiation Therapy

Yifan Shen, *student, Oregon State University,* Nirvik A. Das, *student, Oregon State University,*
Yue Zhang, *Assistant Professor, Oregon State University*
Wolfram Laub, *Clinical Associate Professor, Oregon Health & Science University*

Abstract—Developing an accurate dosage plan for radiation therapy is crucial to the success of the treatment; yet many obstacles still exist in spite of the application of the modern technology. One such challenge is revealed in registering CT scans and MRI images, that capture the location and geometry of the prostate. Due to bodily functions and breathing of the patients, the prostate moves with respect to different images. Relying solely on computer vision techniques such as the demons algorithm, can at best give a quantitative measurement of the differences between images. How the differences are created remains unknown. We develop a pipeline in which we first employ simulations of the movement and deformation of the rectum to depict its influence on the position variation of the prostate, then calculate the displacement fields using demons image registration algorithm, and lastly use the displacement field to correct the simulations to match with the target image. Potentially, physicians can better devise dosage planning knowing how the prostate moves during the treatment.

Index Terms—FEM, prostate, registration, physically based, simulation

1 Introduction

Prostate cancer, is the second most common cause of mortality [1] in the U.S. Almost 20,000 domestic fatalities were reported in the year 2012, according to the statistics published by the American Cancer society [2]. Among the number of treatment methods such as radiotherapy, chemotherapy, hormone therapy and prostatectomy, radiotherapy remains to be a widely used method in practice. One common challenge for physicians is to optimize dosage planning for the cancerous region while minimizing injury to the neighbor organs. We develop a pipeline to include information on how prostate deforms and on the amount of deformation for physicians to improve dosage planning.

To describe prostate movement, we construct 3D volumes of the pelvic section using geometrical data from an anonymized patient collected at Oregon Health and Science University (OHSU). On the geometrical models, we apply biomechanical modeling schemes to deform and move these organs. In the mean time, we implement demons algorithms on different sets of images to obtain the displacement fields based on the intensity variation. Lastly, we utilize these displacement fields to refine our biomechanical models that are developed based on physics. By combining biomechanical modeling and image registration, our simulations can match well with the target images.

We first introduce some technical concepts used in our pipeline in the background section. Then we describe in detail our pipeline. Lastly, we present our numerical results and comparison to CT scans on our patient from OHSU before we conclude in our last section.

- *Yifan Shen, School of Electrical Engineering and Computer Science, Oregon State University, Corvallis, OR, 97330. E-mail: shenyif@oregonstate.edu*
- *Nirvik A. Das, School of Electrical Engineering and Computer Science, Oregon State University, Corvallis, OR, 97330.*
- *Yue Zhang, School of Electrical Engineering and Computer Science, Oregon State University, Corvallis, OR, 97330.*
- *Wolfram Laub, Medical Physics Department, Oregon Health and Science University, Portland, OR, 97239*

Manuscript received October 10, 2016; revised October 10, 2016.

2 Background

Magnetic Resonance Imaging (MRI) [3], used in all radiation therapy, is based on the application of magnetic fields. MRI is commonly used for producing detailed cross sectional images of the human body on any imaging plane. Computer assisted tomography (CT) [4], is another widely used imaging technique that utilizes X-rays to perform scans. The radiation doses for CT are often higher than the regular X-ray modern technology. Typical prostate radiation therapy is delivered on linear accelerators with between 28-42 treatment fractions of 180cGy-250cGy dose each. Typical energies used are between 6MV and 18MV. Intensity Modulated Radiation Therapy (IMRT) is the method of choice. After MRI and CT images have been acquired for a prostate patient, the MRI image data set needs to be registered to the CT scan. This is often done via rigid registration methods or via open-source tools or commercially available tools such as Velocity and Varian that use deformable registration methods.

CT scans often have less soft tissue contrast, while MRI scans can have high contrast soft tissues. But the concern in radiation therapy is image distortion, which can be a problem in MRI imaging. In addition, physicians need the electron density information, which they only get from the CT scans, for heterogeneity calculation when they calculate the dose distribution on patients. For this reason, CT scans are the scans of choice for treatment planning. During patient treatments, physicians at OHSU apply cone beam CTs. By collecting a sequence of images over time, these physicians can then review the treatment progress and

conjecture on cancer growth using 4D data that includes the temporal component. The more the number of data points, the more accurate the diagnosis can be. Our pipeline can potentially provide missing images that are not collected experimentally through numerical modeling.

2.1 Biomechanical Modeling of organs

The number of examples of bio-mechanical models is rising sharply in recent years. Movements in the pelvic region are modeled numerically to develop stabilization of Sacroiliac Joint ligaments, which lead to stability of hips, pelvis and thoracic region [5]. Bladder expansion due to urine inflow was investigated in [6]. Eddie Y.K. et. al. presents a state-of-the-art parallelization technique taking advantage of the unique anatomical fiber architecture of skeletal muscles, describes the use of an indentation test in determination of in vivo mechanical characteristics of human skin and propose the analytical solutions to the mathematical model describing the formation of liver zones via Adomian decomposition method with a system of nonlinear partial differential equations [7]. We also apply continuum mechanics modeling techniques to arrive at a numerical description of prostate movement from bladder and rectum filling [8]. Constitutive equations are created from the balance of the momentum of the physical system, and finite element methods (FEM) that can robustly provide numerical solutions are used as in [9], [10] and [11]. FEM is a method of subdividing a large and complex problem into smaller and simpler parts, that are called finite elements. The simple equations that model these elements are assembled again into a larger system of equations, that model the entire problem. In this way, FEM can find the optimal solution of a complex problem.

To accurately describe the organ materials, experimental measurements that quantify the stress and strain relation for expansion, compression and shear deformations are required. Currently, we use the published hyperelastic material Mooney- Rivlin coefficients from [12], which describes the observed organ tissues behaviors accurately, to describe our organ volumes. The Mooney- Rivlin could be expressed as the following.

$$U = C_{10}(\bar{I}_1 - 3) + C_{01}(\bar{I}_2 - 3) + \frac{1}{D_1}(J_{el} - 1)^2$$

The parameters C_{10}, C_{01} and D_1 define the material properties. Parameter J_{el} denotes the elastic volume ratio. $\bar{I}_1$ and $\bar{I}_2$ are the stress invariants .

To compensate for our current simplification, we employ image registration, which are done to quantify the difference in the organs between two images to refine our numerical modeling of the actual physics. Furthermore, to retain the geometry of the organs from the measured images and scans as accurately as possible, we directly use the point cloud representation. Our results are compared to the commonly used smoothed surfaces in figure 1 (c).

2.2 Demons Image Registration

Image registration is the process of aligning two images based on similarity in intensity patterns or similarity in features. These images could be from multiple sources (multi-modality) or from a single source (mono-modality). A good example of multi-modal registration is registering a CT image and a Positron Emission Tomography (PET) image together. One of the most common algorithms for non-rigid registration is the Demons algorithm and its variants. In 1998, Thirion introduced a suite of algorithms, by considering non-rigid deformable registration as a diffusion process, called the Demons algorithms. The algorithms calculate forces that can be applied to the image pixels to move them, in a way quite similar to how Maxwell calculated demons forces to solve the Gibbs paradox in Thermodynamics [13].

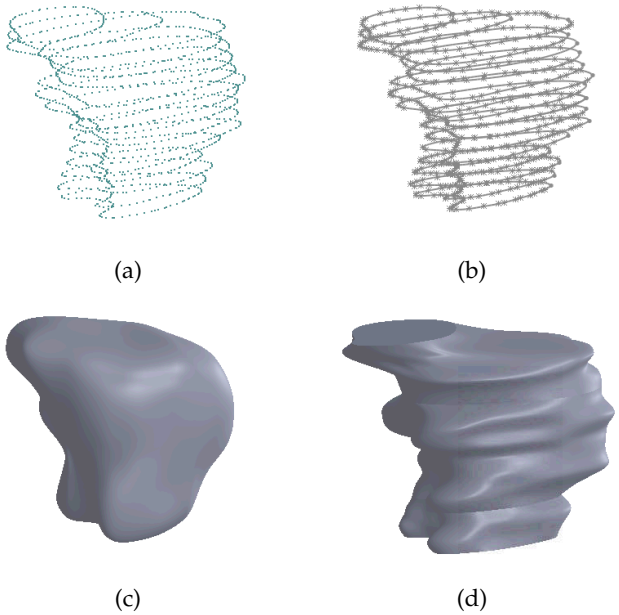

Fig. 1: We demonstrate how we generated 3D volumes of the prostate gland from CT scan data. We connect the contour points of each slice, as shown in image (a). This results in image (b). Image (c) is the result of smoothing the surface. We set boundary surfaces between contour lines to obtain image (d), which is the final approximation of the prostate.

For calculating the demons forces [13], the image to be warped is considered to be the moving image. The target image is considered to be the fixed image. The demons are calculated, based on the principles of diffusion. The forces are given by the following equation:

$$\vec{v} = \frac{(m-s)\vec{\nabla}s}{(\vec{\nabla}s)^2 + (m-s)^2}$$

In the above equation, $\vec{v}$ is the demons force, m is the intensity function of moving image M, s is the intensity function of the static image S and $\vec{\nabla}s$ is the gradient of the fixed/static image S.

The direction of $\vec{v}$ is dependent on the intensities of the points on which the demons are being computed. If the intensity m of a point P is less than the intensity I of the points on the object contour ($m < I$), then the direction is taken to be opposite to the direction of the force on a point with intensity higher than the intensity of the contour point ($m > I$).

Once the displacement field is calculated, the current transformation gets added to the generated displacement field.

$$\phi(x) = x + u(x)$$

Here, $\phi(x)$ refers to the transformation of x after the displacement field gets added to the current transformation. $u(x)$ refers to the displacement field.

3 Our Pipeline

We begin our pipeline by first obtaining the CT scans (CBCT) of an anonymous patient from OHSU for two days. These scans are contoured by the physician into individual organs and tissues. We process these contoured scans using an open-source tool called Computational Environment for Radiotherapy Research (CERR) and extract the contours of interest, i.e. the prostate gland, bladder, the rectum and the pelvic bones. We also make use of the contoured scans to generate some geometric volumes of the organs that are 3D in nature. Once we have obtained the geometric volumes, we perform the FEM simulation of how the organs deform under the influence of biomechanical forces. In the meantime, we perform some image segmentation to filter out the noises from the contours, that were introduced during contouring. We then perform demons registration on these filtered contours of the prostate gland to obtain the displacement field. The displacement field allows us to calculate the force profiles and improve the FEM simulation results.

3.1 Simulation of prostate deformation using FEM

We begin our simulation by first extracting some point clouds from the contours of scans from each day. These point clouds are imported into a 3D modeling software such as Solidworks and processed to create 3D geometric volumes. Once, we have the 3D volumes, we use them in a FEM solver to calculate the deformations between the 3D volumes for the first day and the second day (See Algorithm1).

Algorithm 1 Steps to create the geometric volume and perform FEM simulation

1: **procedure** FEM()
2: *Obtain point clouds from CT scan contours by using CERR*
3: *Import point clouds into SolidWorks to create surfaces and volumes*
4: *Use open source Finite Element numerical solver to design and calculate deformations*

3.2 The displacement field *u*

To deform the second day's 3D volume to first day's 3D volume, we need to get a reference force profile. Using the contours obtained from processing the contoured CT scans, we perform the demon's registration by considering the second day as fixed image and the first day as moving image. This gives us the direction and magnitude of the displacement field (See Algorithm 2).

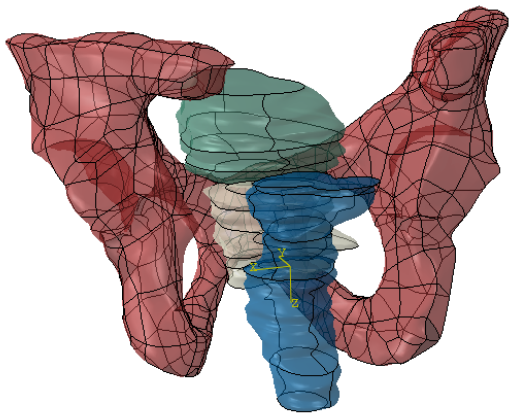

Fig. 2: We demonstrate the 3D volume constructed from the CBCT scans. The red surface represents the pelvic bones which constrains the deformation of the bladder and is considered to be the boundary conditions. The green surface is the bladder. The blue surface is the rectum, which deforms a lot during daily activities and dramatically affects surrounding organs. The beige surface in the middle is the prostate, which is attached to the bladder and close to the rectum.

Algorithm 2 The displacement field u

1: **procedure** DEMONS (FIXED, MOVING)
2: *Fixed image* $\leftarrow$ *Target Image*
3: *Moving image* $\leftarrow$ *Image to be warped*
4: **for** *pyramid level* ≥ 1 **do**
5: *Fixed image* $\leftarrow$ *resized according to scale*
6: *Warped moving image* $\leftarrow$ *resized according to scale*
7: *Calculate the demons on fixed and warped images*
8: *Add displacement field u to current transformation*
9: *Upsample moving and fixed images according to level*
10: $u \leftarrow$ *displacement field*

3.3 Combining FEM simulation and the demons registration

Using the displacement field magnitudes and directions, we calculate the force profiles. We then add them to the 3D volumes along with setting up the boundary conditions, to perform the FEM simulation. We continue iterating the simulations with different force profiles, until we get the desired target 3D volume.

4 Results

Due to soft tissues like blood vessel, membrane and fat, the neighboring organs such as prostate and rectum can slide against one another. This sliding movement is not feasible to be described using the tie interaction property. To test the friction model, we generate a 3D volume, consisting of 2 cubes, a sphere, an ellipsoid and a cylinder to simulate the pelvic bone, prostate, bladder and rectum respectively. We set the interaction property between the bladder and the prostate as a tie connection. We also set the interaction property between the prostate and the rectum to friction.

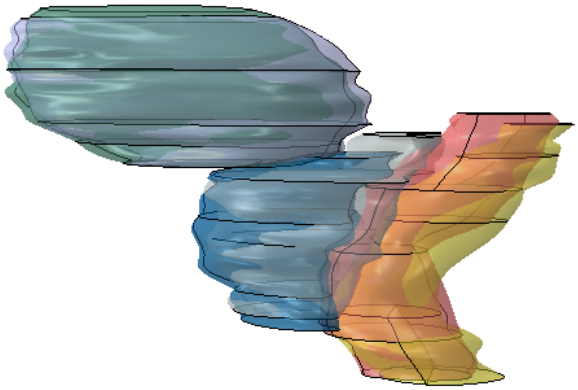

Fig. 3: This image shows the overlapping 3D volumes from both the first and second days. The blue and purple volumes represent the bladder. The blue and beige volumes represent the prostate and the right red and yellow volumes represent the rectum. We find that the prostate deforms a lot due to the rectum filling. In this scenario, the bladder has little effect on the deformation and hence, we focus on the prostate and rectum in our paper.

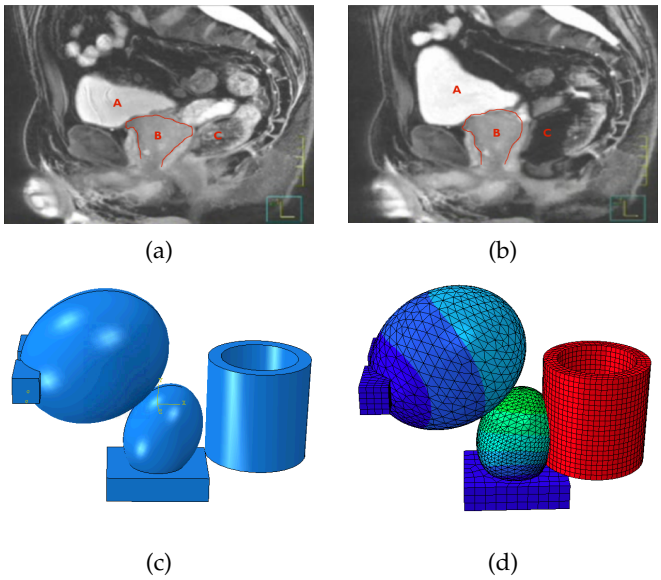

(a) (b)

(c) (d)

Fig. 4: We replicate prostate rotation using simple geometric shapes. Images in the top row are extracted from a video over a two- hour period to show how rectum filling could rotate the prostate and push the bladder. Image (a) is at an earlier time than image (b). The simulation results shown in the bottom row replicates the rotation through an applied pressure inside the rectum wall (cylindrical shell). Image (c) is the undeformed state where the bladder is fixed by a pelvic bone and the prostate is connected to a base that is also fixed. Image (d) shows the deformed state where the prostate is rotated towards the bladder. The total magnitude of the displacement is displayed and the red color indicates the largest displacement, while the blue is the smallest.

Then we move the rectum and observe the deformation (See figure 4). Using this test allows us to observe the effects of rectum filling on the prostate gland, due to the friction property. Testing the simple model gives us a generalized idea on how the prostate reacts to the rectum filling, which aids us in simulating the actual 3D volume. In our case, the prostate rotates under the influence of the rectum filling (See figure 3).

We obtain 88 CT slices of the anonymous patient, per day. These slices are horizontal in nature. Using the contour points of these horizontal CT slices, the 3D volumes are constructed. We use Matlab to process the contoured scans and filter them for noises. Since, the registration process is sensitive to intensity, we had to ensure that the thickness of the contour is reduced as much as possible by filtering them for noises. The resulting contours of the prostate gland are as shown in the figure 6 (a) and figure 6 (b). Once we have these contours, we implement the demons registration to compute the displacement field. The displacement field obtained from the registration of the first and second day scans is shown in figure 6. The figures represent the direction in which the displacement vectors are acting.

We deform the second day's prostate (moving image) to the first day's prostate (fixed image), by expanding the rectum, as if it is getting filled. We perform the FEM simulation to obtain the second day's deformed prostate after the first iteration (See figure 7). Our simulation provides the missing frames the first day to the second day that we observe in a video demonstrating how a filled up rectum pushes the prostate. Once we perform the registration, we obtain the displacement field magnitude and direction. Figure 7 also shows the overlapping comparison of the first day and second day. We can see the volume difference at the right side of the prostate in figure 7 (g). We can observe the overlapping image of the first iteration result (covered by the mesh) and the first day's prostate (shown in blue). After the first iteration, the volume difference is reduced. We use the displacement field and calculate the force profile for the second iteration of the simulation. As observed, figure 7 (g) is the improved result. We find that the improved simulation result is much more closer to the first day's prostate.

This procedure can be carried out for all slices. We choose particular slices in order to improve our FEM simulation. Anatomically, it is known to us that the malignant tumor is usually towards the side of the prostate gland that is in contact with the rectum. As seen in figure 3, the prostate rotates forward due to rectum filling. When the prostate rotates, the tumor moves forward, making it difficult for the physicians to observe the tumor. Our pipeline produces finer results that can aide the physicians to track the deformed prostate and treat the tumor accordingly.

5 Discussion and Conclusions

Registering MRI and CT images provides vital information for researchers and physicians to design successful treatment plans for radiation therapy. Numerical modeling of movement of the prostate gland, due to bladder and rectum filling, can reveal information to adjust and improve the dosage planning.

We test our pipeline using rectum filling and simulating how it affects the deformation of the prostate. Some of the limitations we encountered during the experiment involves

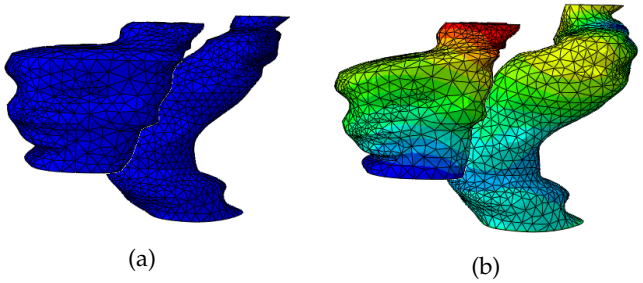

(a) (b)

Fig. 5: We display how the deformation takes place as a result of rectum filling. Image (a) shows the undeformed prostate and rectum. Image (b) shows the outcome of simulating FEM. The red color means largest displacement, and the blue means the smallest displacement.

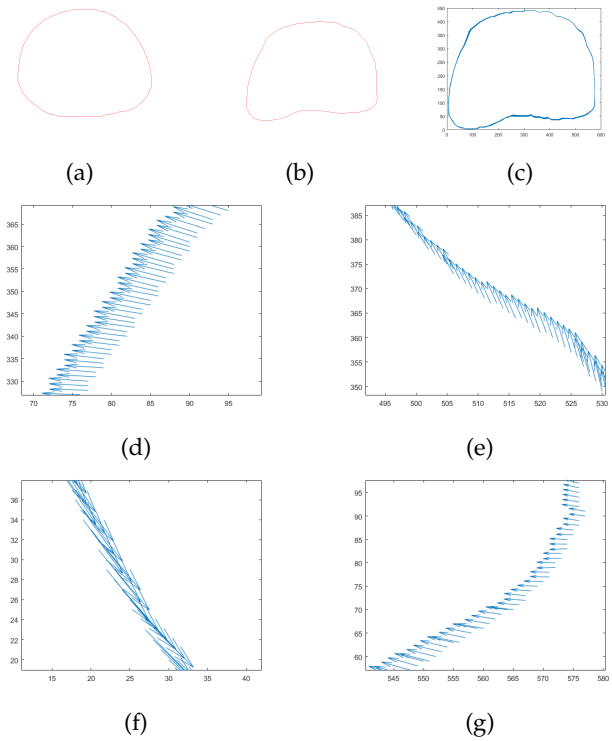

(a) (b) (c) (d) (e) (f) (g)

Fig. 6: We perform the demons registration for slice 14, each from the first day and the second day. Image (a) gives us the contour of the scan from first day (fixed). Image (b) gives us the contour of the second day (moving). Registering images (a) and (b) results in the displacement field direction vectors as shown in image (c), which is necessary for calculating the force profiles. Images (d), (e),(f) and (g) represent the magnified versions of the displacement field direction vectors on top-left, top-right, bottom-left and bottom-right respectively.

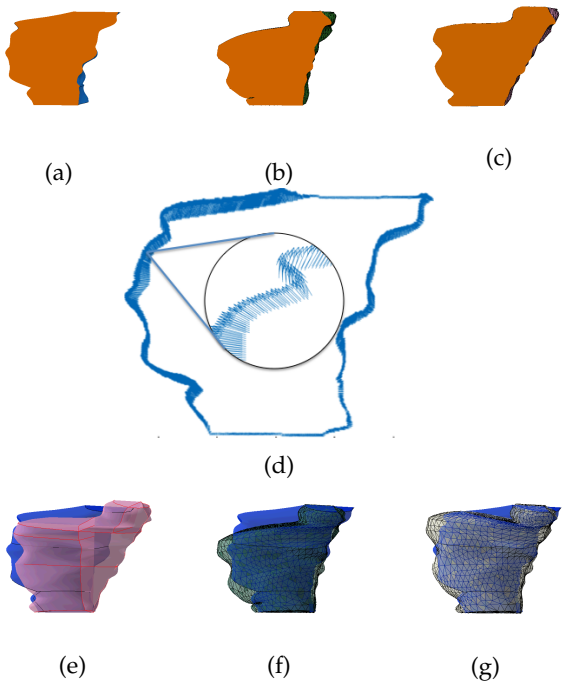

(a) (b) (c) (d) (e) (f) (g)

Fig. 7: We demonstrate the result of using demons registration to aid the simulation of prostate deformation. We deform the second days prostate (moving image) to the first days prostate (fixed image). Image (a) represents the first days prostate. Image (b) is the second days deformed prostate after the simulation of rectum filling. Image (c) is the second days prostate. Image (d) is the displacement field from the demons registration. Image (e) is the overlapping comparison of the first day's prostate (shown in blue) and second day's prostate (shown in pink). We can observe the volume difference at the right side of the prostate. Image (f) shows the overlapping image of deformed prostate (covered by the mesh) which is caused by rectum filling and the first days prostate (shown in blue). After the rectum filling simulation, the volume difference reduces. Then we use the displacement field from image (d) and calculate the force profile for the second iteration of the simulation. We observe that the improved simulation result (shown in grey mesh) which is shown in image (g) is much more closer to the first day's prostate (shown in blue).

not having an anchor point to get controlled displacement fields, lacking of accuracy in differentiating between the organs and surrounding tissues and considering the effects on the prostate due to the surrounding tissues and bladder filling.

In our future work, we are going to work on calculating the anchor point. Currently, our pipeline does not make use of an anchor point, and thus the displacement fields become susceptible to inconsistencies and variations upon calculations. Using an anchor point would allow us to control how the displacement fields are calculated.

Once we complete the simulation of the entire pelvic section, we can predict the maximum prostate rotation and movement under various bladder and rectum filling conditions. Knowing the maximum change in prostate, treatment

plans can include some practical error margins. These error margins would be helpful for the physicians, as they would be able to make better estimations during dosage planning.

ACKNOWLEDGEMENTS

The authors would like to thank Dr. Stephanie Junell, a Medical Physics Physicist at Oregon Health and Science University for the contours delineation.

REFERENCES

[1] J. Ferlay, F. Bray, P. . Pisani, and D. Parkin, "Cancer incidence, mortality and prevalence worldwide, version 1.0," *IARC CancerBase*, no. 5, 2001.

[2] A. C. Society, "Cancer facts figures 2016, 2016," *Atlanta: American Cancer Society*, 2016.

[3] K.-H. Ng, A. C. Ahmad, M. Nizam, and B. Abdullah, "Magnetic resonance imaging: Health effects and safety," in *Proceedings of the international conference on non-ionizing radiation at UNITEN (ICNIR2003) electromagnetic fields and our health*, 2003.

[4] D. J. Brenner and E. J. Hall, "Computed tomographyan increasing source of radiation exposure," *N Engl J Med*, vol. 357, pp. 2277–84, 2007.

[5] J. Pel, C. Spoor, A. Pool-Goudzwaard, G. H. van Dijke, and C. Snijders, "Biomechanical analysis of reducing sacroiliac joint shear load by optimization of pelvic muscle and ligament forces," *Annals of biomedical engineering*, vol. 36, no. 3, pp. 415–424, 2008.

[6] X. Chai, M. van Herk, J. B. van de Kamer, M. C. Hulshof, P. Remeijer, H. T. Lotz, and A. Bel, "Finite element based bladder modeling for image-guided radiotherapy of bladder cancer," *Medical physics*, vol. 38, no. 1, pp. 142–150, 2011.

[7] E. Y. Ng, H. S. Borovetz, E. Soudah, and Z. Sun, "Numerical methods and applications in biomechanical modeling," *Computational and mathematical methods in medicine*, vol. 2013, 2013.

[8] G. Holzapfel, *Nonlinear Solid Mechanics, a Continuum Approach*. John Wiley and Sons, LTD, 2006.

[9] G. Nikishkov, "Introduction to the finite element method," *University of Aizu*, 2004.

[10] G. Strang and G. J. Fix, *An analysis of the finite element method*. Prentice-hall Englewood Cliffs, NJ, 1973, vol. 212.

[11] T. J. Hughes, J. A. Cottrell, and Y. Bazilevs, "Isogeometric analysis: Cad, finite elements, nurbs, exact geometry and mesh refinement," *Computer methods in applied mechanics and engineering*, vol. 194, no. 39, pp. 4135–4195, 2005.

[12] "Finite element modeling of interactions between pelvic organs due to pressure," in *10e colloque national en calcul des structures*, 2011, pp. Clé–USB.

[13] J.-P. Thirion, "Image matching as a diffusion process: an analogy with maxwell's demons," *Medical image analysis*, vol. 2, no. 3, pp. 243–260, 1998.